

Cost-Effective ECC with Low Fiber Content for Pavement Application

Gabriel Arce^{1,*}, Hassan Noorvand¹, Marwa Hassan¹, Tyson Rupnow², and Ricardo Hungria¹

¹Department of Construction Management, Louisiana State University, Baton Rouge, LA

²Louisiana Transportation Research Center, Louisiana State University, Baton Rouge, LA

Abstract. The objective of this study was to evaluate the feasibility of a cost-effective Engineered Cementitious Composite (ECC) with low fiber content (1.5% volume fraction) for pavement application. The ECC material studied was evaluated in compression, uniaxial tension and bending. In addition, flexural fatigue performance was evaluated. The cost-effective ECC material evaluated in this study exhibited a compressive strength of 37.6 MPa, a tensile ductility of 2.61%, and a flexural strength of 9.58 MPa. Moreover, the ECC material exhibited an equivalent flexural fatigue life to that of concrete at approximately two times the applied stress. Based on the experimental findings, it was shown that the cost-effective ECC materials with low fiber content can be promising for pavement application.

1 Introduction

Recently, engineered cementitious composites (ECC) have been proposed as an alternative material for the construction of jointless rigid pavements and overlays [1-4]. ECC are novel fiber reinforced cementitious materials that possess high tensile ductility, in the order of 100 to 500 times that of regular concrete (between 1 to 5% strain capacity in tension) [5]. In uniaxial tension, ECC materials exhibit a “yield point” (as the first crack of the cementitious matrix occurs at about 0.01% strain) with a subsequent strain-hardening behavior (increase in load carrying capacity with further deformation). This strain-hardening behavior occurs by the formation of multiple microcracks and is known as Pseudo Strain-Hardening (PSH) [6]. Microcracks open from zero to about 60 μm between the first-cracking strain (of about 0.01%) and 1% strain where further deformation causes more microcracks formation without additional crack opening [6-8]. This steady-state crack width is an intrinsic property of the material (which can be adjusted with the use of micromechanics concepts) and is fundamental to the great durability potential of these novel materials [6].

Research on ECC durability has shown promising results against major types of concrete deterioration including corrosion, freeze-thaw, alkali silica reaction and sulfate attack [6, 9, 10]. Furthermore, ECC exhibits significant self-healing characteristics because of its tight crack width that allows autogenous healing mechanisms of cementitious materials to be effective; thus, enhancing durability potential of this novel material even more [11, 12]. To date, ECC have been applied in bridge deck link slabs, bridge deck patches, and several repairs of concrete structures with successful performance [6, 13, 14].

While ECC properties are promising for pavement and overlay applications, its high cost limits its implementation. ECC typically utilizes 2% volume fraction of polyvinyl alcohol (PVA) fiber, microsilica sand, and high contents of cement, which greatly increase its cost (especially PVA fiber) compared to typical concrete. This paper focuses on the evaluation of low fiber content PVA-ECC utilizing locally available fine river sand and a high level of cement replacement with fly ash to enhance the cost-effectiveness and practicality of ECC in pavement applications. The PVA fiber selected in this study is a low-cost PVA fiber (non-oil coated) readily available in the US.

2 Background

ECCs are a special type of High-Performance Fiber Reinforced Cementitious Composite (HPFRCC) designed and optimized by the utilization of micromechanics concepts to exhibit PSH (as shown in Figure 1a) at relatively low fiber contents [15]. There are two basic conditions that need to be met for the PSH behavior to occur, the strength criterion and the energy criterion [7]. The strength criterion (Eq. 1) guarantees adequate fiber-bridging capacity upon crack initiation and requires the first-cracking strength of the composite to be less than the fiber-bridging capacity on any plausible crack plane [7]. On the other hand, the energy criterion (Eq. 2) provides for steady-state flat crack propagation, which occurs when the crack tip matrix toughness (J_{tip}) is less or equal than the complementary energy of the fiber bridging relation (J_b) as demonstrated by Marshall and Cox utilizing J-integral analysis [6, 7, 16].

- Strength criterion [6]:

* Corresponding author: garceal@lsu.edu

$$\sigma_0 \geq \sigma_{cs} \quad (1)$$

where,
 σ_0 = Maximum fiber-bridging capacity;
 σ_{cs} = Cracking strength.

- Energy Criterion [6]:

$$J'_b = \sigma_0 \delta_0 - \int_0^{\delta_0} \sigma(\delta) d\delta \geq J_{tip} \quad (2)$$

where,
 J'_b = Complementary energy of the fiber-bridging relation;
 J_{tip} = Crack tip matrix toughness;
 δ_0 = Crack opening corresponding to σ_0 ;
 $\sigma(\delta)$ = Fiber-bridging relationship.

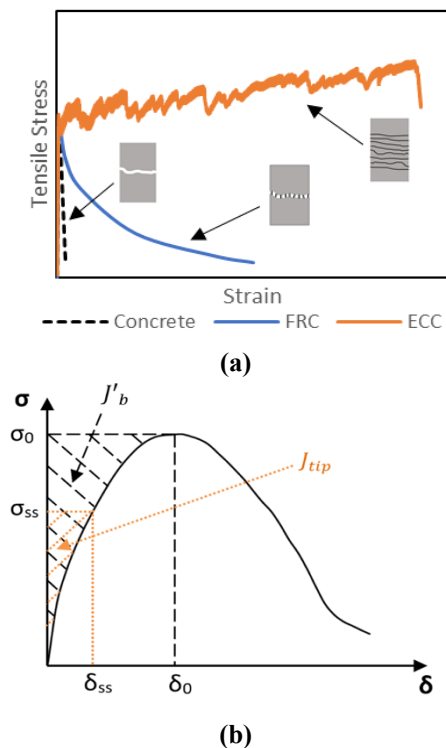


Fig. 1. (a) Stress vs. strain behavior of cementitious materials (b) fiber bridging relation (σ - δ curve).

If the crack tip matrix toughness (sensitive to the details of the cementitious matrix design such as water/binder ratio, cement replacement with fly ash and aggregate type) is too high or inadequate occur in the increasing phase of the σ - δ curve, then, steady-state crack propagation is hard to be achieved [17, 18]. Figure 1b presents a graphical representation of and on a schematic fiber-bridging curve.

From Eqs.1 and 2, successful design of ECC is achieved when both the strength and the energy criteria are satisfied. Consistent with the conditions for PSH behavior presented above, if the ratios σ_0/σ_{cs} and J'_b/J_{tip} pseudo strain-hardening performance indexes (PSH indexes) are greater than one then, both, the strength and the energy criteria will be met. Otherwise, if any of the two ratios are less than one, the tensile-softening

behavior of fiber reinforced concrete (FRC) will prevail (as shown in Figure 1a).

3 Objectives

The objective of this study was to evaluate the properties of a low cost Engineered Cementitious Composite (ECC) with low fiber content (1.5% volume fraction), locally-available fine river sand (instead of microsilica sand), and high replacements of cement with fly ash (75% by weight) for pavement applications.

4 Experimental program

4.1 Materials

Locally-available ingredients were utilized to reduce the cost of ECC: Ordinary Portland Cement (OPC) Type I, Class F Fly Ash (FA), and fine river sand with a maximum particle size of 1.18 mm and a fineness modulus of 1.96. Chemical compositions of cement and FA are presented in Table 1 according to XRF analysis.

Table 1. Chemical composition of cement & fly ash (Wt %).

| Material | Cement | Fly ash |
|--------------------------------|--------|---------|
| SiO ₂ | 19.24 | 51.12 |
| Al ₂ O ₃ | 4.75 | 20.87 |
| Fe ₂ O ₃ | 3.35 | 5.81 |
| CaO | 65.81 | 14.55 |
| MgO | 2.20 | 2.21 |
| SO ₃ | 3.61 | 0.95 |
| K ₂ O | 0.54 | 1.26 |
| TiO ₂ | 0.21 | 1.70 |

Fibers utilized throughout the investigation were non-oil-coated polyvinyl alcohol (PVA) fibers. Table 2 present the properties of the PVA fibers utilized. Moreover, a polycarboxylate-based High Range Water Reducer (HRWR) was utilized as admixture.

Table 2. PVA fibers properties.

| Fiber Type | RECS 15 |
|------------------------------|---------|
| Length (mm) | 8 |
| Diameter (μm) | 38 |
| Young's Modulus (GPa) | 40 |
| Tensile Strength (MPa) | 1600 |
| Elongation (%) | 5.7 |
| Density (g/cm ³) | 1.3 |

4.2 Specimen preparation

Cylindrical, dog-bone shaped, and prismatic specimens were cast to evaluate the compressive, tensile, and flexural properties of the ECC mixture M3-1.5% after 3, 7 and 28 days of curing as shown in Table 3. The M3-1.5% mixture proportions are summarized in Table 4.

Table 3. Experimental matrix.

| Age | Number of Specimens | | | |
|---------|---------------------------|-----------------------|---------------------------|-----------------------|
| | Compressive Strength Test | Uniaxial Tensile Test | Flexural Performance Test | Flexural Fatigue Test |
| 3 Days | 3 | 6 | 3 | - |
| 7 Days | 3 | 6 | 3 | - |
| 28 Days | 3 | 9 | 5 | 9 |

Table 4. ECC mixture design proportions by weight.

| Mix ID | M3-1.5% |
|-----------------------|---------|
| Cement | 1 |
| Fly Ash | 3.0 |
| Water | 1.09 |
| Sand | 1.45 |
| HRWR (%) ¹ | 0.13 |
| W/B | 0.27 |
| S/B | 0.36 |
| FA/C | 3.0 |
| FA (%) ² | 75 |
| Fibers (Vol %) | 1.50 |

¹%HRWR dosage by weight of cement

²% of cement replacement with fly ash by weight

The ECC mixing procedure consisted of the following steps. Dry powder components (cement and fly ash) were mixed in a planetary mixer for three minutes. Sand was then combined with the dry powders and mixed for three additional minutes. Subsequently, water and HRWR were added and mixed for three additional minutes. Next, the rheology of the mixture was assessed by means of the modified marsh funnel test proposed by Li and Li [19]. In this study, the consistency of the mixture design was controlled to exhibit a flow number between 14 and 18 seconds. Finally, PVA fibers were introduced slowly to the wet mixture (for 3 min) and mixed for an additional 7 minutes.

Specimens prepared were demolded after 24 hours of casting (specimens were covered with plastic to prevent

moisture loss) and then allowed to cure for 28 days in water saturated with calcium hydroxide at a controlled temperature of $23 \pm 2^\circ\text{C}$ according to ASTM C 511.

4.3 ECC testing

4.3.1 Compressive strength

The compressive strength of the ECC was evaluated according to ASTM C 39 on 101.6 x 203.2 mm (4 in x 8 in) cylindrical specimens. As shown in Table 3, specimens were prepared to measure the compressive strength of the ECC material at 3, 7 and 28 days. The experimental tests were performed by means of hydraulic pressure with a constant loading rate of 0.25 MPa/s.

4.3.2 Uniaxial tensile test

To characterize the tensile behavior of the ECC material, uniaxial tensile tests were conducted on dog-bone shaped specimens per recommendations of the Japan Society of Civil Engineers [20]. As shown in Table 3, dog-bone shaped specimens were cast to perform the uniaxial tensile test at 3, 7 and 28 days of curing. A schematic of a dog-bone shaped specimen is shown in Figure 2a. The tensile tests were carried out using a 250-kN capacity servo-hydraulic machine under displacement control and at a loading rate of 0.5 mm/min. To measure the deformation, two LVDTs were attached to each side of the specimens as illustrated in Figure 2b.

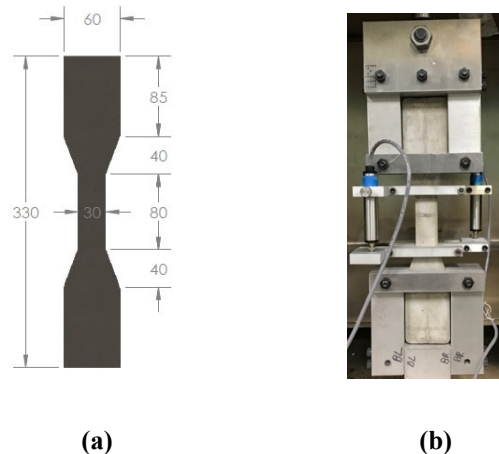


Fig. 2. (a) Dog-bone shaped specimen dimensions (b) uniaxial tensile test setup.

4.4 Third point bending test

Third-point bending test was conducted according to ASTM C 1609 using a closed-loop, servo-hydraulic universal testing system to assess the flexural strength and deformation capacity of the ECC material evaluated. Prismatic specimens having dimensions of 101.6 x 101.6 x 355.6 mm (4 x 4 x 14 in) were cast to evaluate the flexural performance of the ECC material after 3, 7 and

28 days of curing. A span length of 300 mm with center span length of 100 mm was used for flexural loading. The load was applied at a rate of 0.075 mm/min. Mid-span beam net deflection and load were recorded on an automated information recording system during the third-point bending test. To measure the deflection of ECC specimens, two linear variable displacement transducer (LVDT) were attached to the testing set-up as shown in Figure 3.



Fig. 3. Third-Point Bending Testing Setup.

4.4.1 Flexural fatigue test

Flexural fatigue test was conducted on the same setup than ASTM C 1609 (as shown in Figure 3); yet, without attachment of LVDTs. Cyclic loading was applied in a sinusoidal waveform at a frequency of 5 Hz. The stress ratios (ratio between the maximum applied flexural stress, σ_{max} and the flexural strength of the material) evaluated were 0.9, 0.8, & 0.7. Moreover, the minimum flexural stress (σ_{min}) was sustained at 20% of σ_{max} .

5 Results and analysis

5.1 Compressive strength

Figure 4 presents the compressive strength results of the M3-1.5% ECC material at different stages of curing. As expected, the compressive strength of the ECC increased with curing progression. At 28 days, the compressive strength reported was 37.6 MPa which is significantly greater than that of normal strength concrete (30 MPa). In addition, the relative strength (compared to the 28-day strength) at 3 and 7 days of curing (39.4% and 58.0%, respectively) was comparable to that of regular concrete.

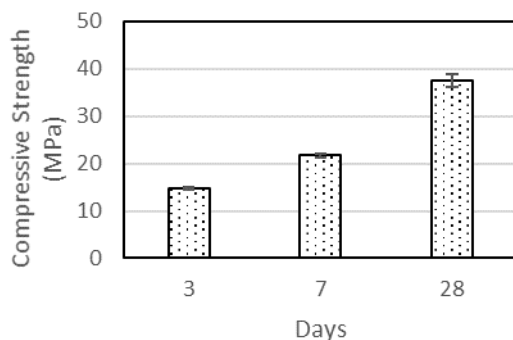
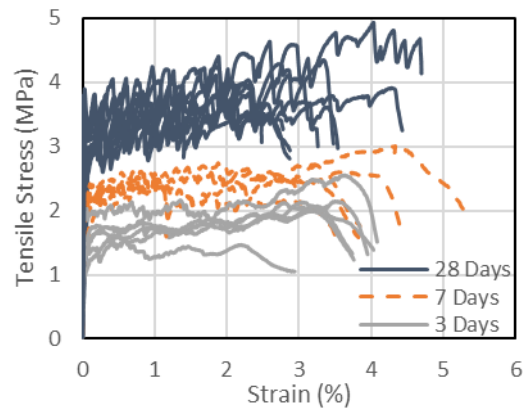


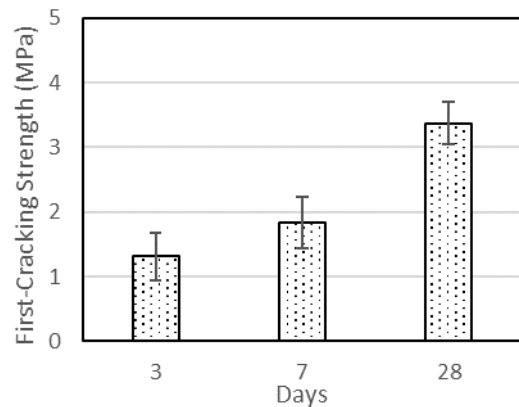
Fig. 4. Compressive strength results.

5.2 Uniaxial tensile test

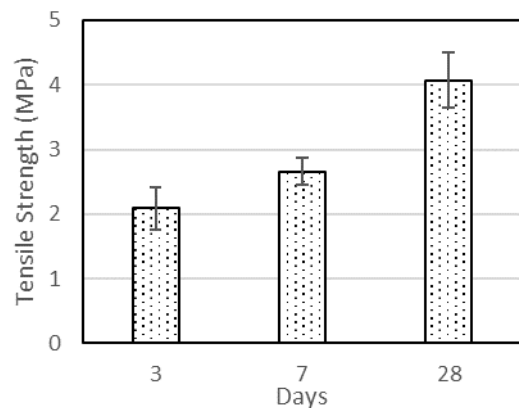
Figure 5a presents the tensile stress vs. strain curves of M3-1.5% ECC at different stages of curing. As shown in this figure, the ECC material exhibited PSH behavior after the first-cracking strength was reached producing significant amounts of deformation with an increase in load carrying capacity. However, a tradeoff between ductility and strength was observed with curing progression (as shown in Figure 5).



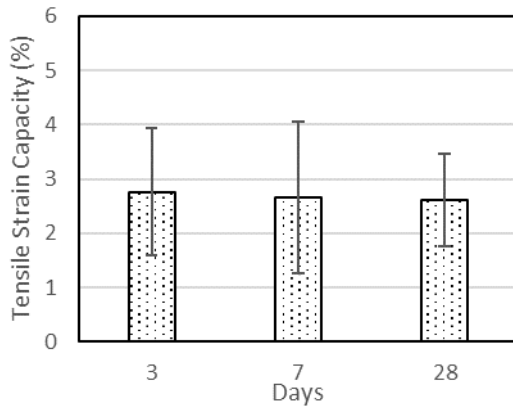
(a)



(b)



(c)



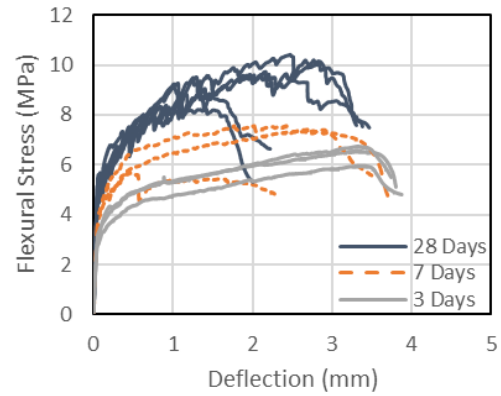
(d)

Fig. 5. Uniaxial Tensile Test Results (a) Tensile Stress vs. Strain Curves (b) First-Cracking Strength (c) Tensile Strength (d) Tensile Strain Capacity.

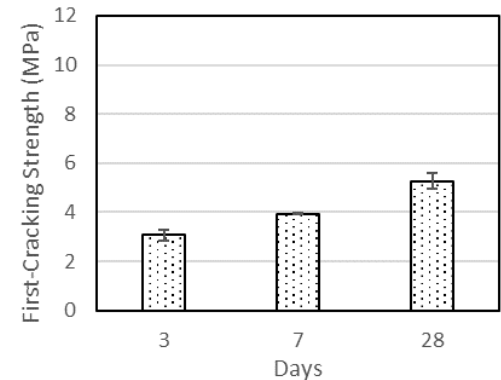
The decrease in tensile ductility with the progression of curing is closely related to the pseudo strain hardening performance indicators PSH strength (σ_0/σ_{cs}) and PSH energy (J_b/J_{tip}). As curing progresses the cementitious matrix of the ECC material is strengthened. In turn, the crack-tip toughness (J_{tip}) and cracking strength (σ_{cs}) of the cementitious matrix increases; thus, producing a reduction in both PSH strength (σ_0/σ_{cs}) and PSH energy (J_b/J_{tip}) indexes leading to the observed decrease in ductility [21]. On the other hand, as curing progresses the bond between the fibers and the cementitious matrix is enhanced. Consequently, the superior fiber/matrix interface produces an increase in the fiber bridging capacity (σ_0) yielding an increase in the tensile strength of the composite. After 28 days of curing, the strain capacity of the M3-1.5% ECC material was 2.61% which is orders of magnitude superior to that of regular concrete (261 times that of regular concrete).

5.3 Flexural performance

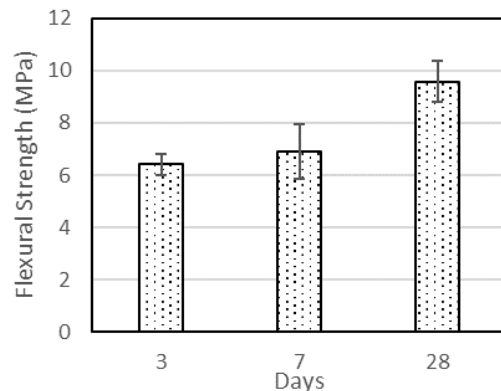
Figure 6a presents the flexural Stress vs. deflection curves of M3-1.5% ECC at different stages of curing. As expected, the ductile tensile behavior of M3-1.5% ECC was reflected in the flexural performance of the beam specimens. At all curing stages, M3-1.5% exhibited a PSH behavior after the first-cracking strength was reached producing significant amounts of deformation with an increase in load carrying capacity. Moreover, similarly to the phenomena observed in the uniaxial tensile test, a tradeoff between deflection capacity and flexural strength was observed with curing progression (as shown in Figure 6). The decrease in deflection capacity and increase in flexural strength with the progression of curing is attributed to the same phenomena discussed in the uniaxial tensile test section above. After 28 days of curing, the flexural strength of the M3-1.5% ECC material was 9.58 MPa which is approximately two times that of regular concrete.



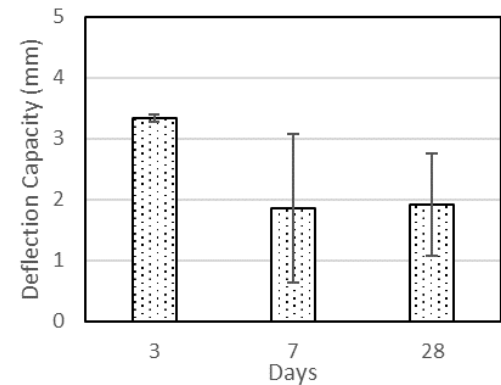
(a)



(b)



(c)



(d)

Fig. 6. Flexural performance (a) flexural stress vs. deflection curves (b) first-cracking strength (c) flexural strength (d) deflection capacity.

5.4 Flexural fatigue

Flexural fatigue performance of concrete materials is key for the design of rigid pavements. For this reason, flexural fatigue testing of M3-1.5% ECC material was conducted. Figure 7 presents the S-N curves for M3-1.5% ECC and normal concrete. The concrete data was obtained from a study by Oh [22]. As shown in Figure 7, under cyclic loading M3-1.5% ECC exhibits a remarkably better performance than that of concrete. For the same fatigue life, M3-1.5% ECC can be subjected to approximately two times the flexural fatigue stress than concrete. In turn, this can allow for substantial thickness reduction and enhanced durability of pavements constructed utilizing M3-1.5% ECC.

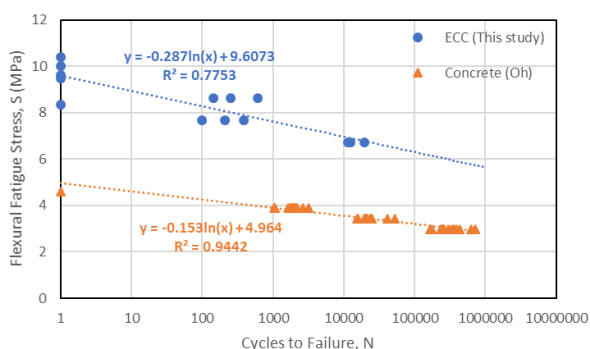


Fig. 7. Flexural fatigue stress vs. cycles to failure curve for ECC and concrete.

6 Conclusions

Based on the experimental findings of this study, it was shown that cost-effective ECC materials manufactured with low fiber content (1.5% volume fraction), such as M3-1.5%, are promising for pavement application due to their remarkable mechanical properties. After 28 days of curing M3-1.5% ECC exhibited a compressive strength of 37.6 MPa (significantly greater than that of normal strength concrete), a tensile ductility of 2.61% (261 times that of concrete), and a flexural strength of 9.58 MPa (approximately two times that of concrete). In addition, flexural fatigue performance of ECC M3-1.5% was shown to be substantially superior to that of regular concrete with M3-1.5% achieving an equivalent fatigue life to that of concrete at approximately two times the applied stress.

References

1. Qian, S., and Li, V.C., (2008). Durable Pavement with ECC. 1st International Conference on Microstructure Related Durability of Cementitious Composites, (October), 535–543.
2. Zhang, Z., Zhang, Q., Qian, S., and Li, V.C., (2015). Low E Modulus Early Strength Engineered Cementitious Composites Material. Transportation Research Record: Journal of the Transportation Research Board, **2481**, 41–47.

3. Zhang, Z., Hu, J., and Ma, H., (2017a). Feasibility study of ECC with self-healing capacity applied on the long-span steel bridge deck overlay. International Journal of Pavement Engineering, **8436**(September), 1–10.
4. Zhang, Z., Qian, S., Liu, H., and Li, V.C., (2017b). Ductile concrete material with self-healing capacity for jointless concrete pavement use. Transportation Research Record Journal of the Transportation Research Board, **734**, 1–12.
5. Li, M.L. and V.C., (2009). Influence of Material Ductility on Performance of Concrete Repair. ACI Materials Journal, 419–428.
6. Li, V.C., (2008). Engineered Cementitious Composites (ECC) – Material, Structural, and Durability Performance. Concrete Construction Engineering Handbook, **78**.
7. Ma, H., Qian, S., Zhang, Z., Lin, Z., and Li, V.C., (2015). Tailoring Engineered Cementitious Composites with local ingredients. Construction and Building Materials, Elsevier Ltd, **101**, 584–595.
8. Sahmaran, M., Lachemi, M., Hossain, K.M.A., Ranade, R., and Li, V.C. (2009). Influence of aggregate type and size on ductility and mechanical properties of engineered cementitious composites. ACI Materials Journal, **106**(3), 308–316.
9. Liu, H., Zhang, Q., Li, V., Su, H., and Gu, C., (2017). Durability study on engineered cementitious composites (ECC) under sulfate and chloride environment. Construction and Building Materials, Elsevier Ltd, **133**, 171–181.
10. Sahmaran, M., and Li, V.C., (2016). Suppressing Alkali-Silica Expansion. Concrete International, 47–52.
11. Şahmaran, M., Yildirim, G., Noori, R., Ozbay, E., and Lachemi, M., (2015). Repeatability and Pervasiveness of Self-Healing in Engineered Cementitious Composites. ACI Materials Journal, **112**(4), 513–522.
12. Yang, Y., Lepech, M. D., Yang, E. H., and Li, V.C., (2009). Autogenous healing of engineered cementitious composites under wet-dry cycles. Cement and Concrete Research, **39**(5), 382–390.
13. Li, V.C. (2003). On engineered cementitious composites (ECC). A review of the material and its applications. Journal of Advanced Concrete Technology, **1**(3), 215–230.
14. Qian, S., Lepech, M. D., Kim, Y.Y., and Li, V.C., (2009). Introduction of transition zone design for bridge deck link slabs using ductile concrete. ACI Structural Journal, **106**(1), 96–105.
15. Li, V.C. (1993). From Micromechanics Engineering Design for Compo- of Cementitious Engineering. JSCE Journal of Structural Mechanics Earthquake Eng., **471**(I-24), 37s–48s.
16. Marshall, D.B., and Cox, B. N. (1988). A J-integral method for calculating steady-state matrix cracking

- stresses in composites. *Mechanics of materials*, **7**(2), 127–133.
17. Li, V.C., Wu, C., Wang, S., Ogawa, A., and Saito, T., (2002). Interface tailoring for strain-hardening polyvinyl alcohol-engineered cementitious composite (PVA-ECC). *ACI Materials Journal*, **99**(5), 463–472.
 18. Pan, Z., Wu, C., Liu, J., Wang, W., and Liu, J. (2015). Study on mechanical properties of cost-effective polyvinyl alcohol engineered cementitious composites (PVA-ECC). *Construction & Building Materials*, **78**, 397–404.
 19. Li, M., and Li, V.C. (2013). Rheology, fiber dispersion, and robust properties of Engineered Cementitious Composites. *Materials and Structures*, **46**(3), 405–420.
 20. Japan Society of Civil Engineers. (2008). Recommendations for Design and Construction of High Performance Fiber Reinforced Cement Composites with Multiple Fine Cracks (HPFRCC). Concrete Engineering Series, **82**, Testing Method 6-10.
 21. Li, V.C. (2012). Tailoring ECC for Special Attributes: A Review. *International Journal of Concrete Structures and Materials*, **6**(3), 135–144.
 22. Oh, B.H. (1991). Fatigue-Life Distributions of Concrete for Various Stress Levels. *ACI Materials Journal*, **88**(2), 122–128.